

## CHAPTER 5

### RESULTS AND DISCUSSION

The consistency and reliability of NN fatigue life prediction using the Levenberg-Marquardt algorithm for various polymeric composites will be presented in this chapter by comparing the predicted results with the corresponding experimental or simulated data. For better insights, the comparisons are also presented in the form of the classical  $S$ - $N$  curve. Using the algorithm scheme, the associated NN regularization parameters  $\alpha$  and  $\beta$  are adjusted automatically and updated iteratively during the NN iterations. Discussion on the results are then presented accordingly. Finally, the quality of the NN fatigue life prediction is assessed systematically.

#### 5.1 NN Fatigue Life Prediction

The following fatigue life prediction results have been collected based on the NN parameters and stopping criteria listed in Table 5-1.

**Table 5-1** NN parameters used in the modeling study

| NN Parameter                                 | Value               |
|----------------------------------------------|---------------------|
| initial lambda, $\lambda_{\text{init}}$      | 0.005               |
| initial weight decay, $\alpha_{\text{init}}$ | 0                   |
| initial inverse noise, $\beta_{\text{init}}$ | 1                   |
| maximum number of iterations                 | 200                 |
| minimum gradient, $\mathbf{g}_{\text{min}}$  | $1 \times 10^{-10}$ |
| maximum lambda, $\lambda_{\text{max}}$       | $1 \times 10^{10}$  |
| performance goal                             | 0                   |
| number of hidden nodes, $s$                  | 10                  |

Before the NN prediction results are presented, the NN model output during the training phase is presented first to show how the NN responded during the phase. Since all of the

training phase results are similar for all the materials, only the training phase results of Material I is shown in Figure 5-1 for training set of 0.1 and -2 with MSE of 0.000188.

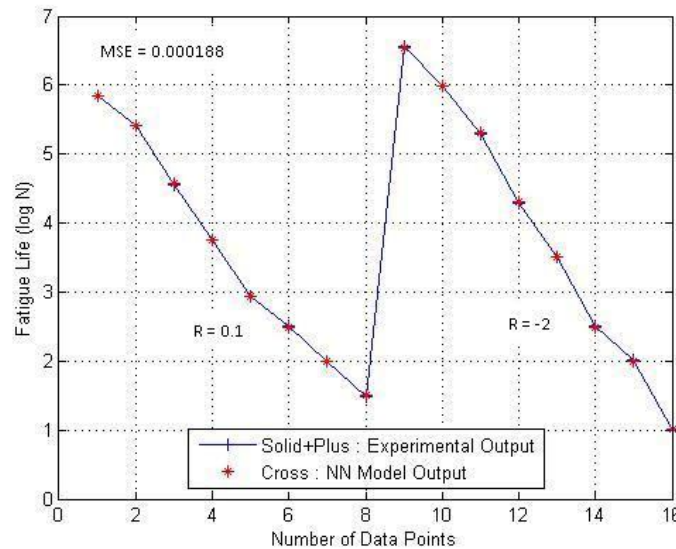


**Figure 5-1** The NN training output for Material I with training set of  $R = 0.1$  and  $-2$ .

Note that only two out of the three lines in Figure 5-1 are representing experimental data trend (the first and third lines). The second line has no meaning except for plotting continuity. In addition, the associated cross marks are indicating the NN prediction trend. These clarifications on the model output hold throughout the thesis.

From the proximity of both the experimental data trend and prediction trend, the quality of the NN model output can be assessed. Further, the quality of the NN model output can be quantified by calculating the mean square error (MSE) between the two trends.

Looking at Figure 5-1, it can be seen that commonly NN fits well to the training examples as indicated by both the close match of the experimental data and NN output, and a small MSE value of 0.000188. After the training phase, the NN model response is checked and tested in predicting fatigue life based on new fatigue data at other stress ratios- $R$  than that used in the training phase. For example, for Material I, stress ratios of 0.1 and -2 were employed in the training phase while stress ratios of -0.5, -1, 0.5 and 10 were used in the testing phase.

### 5.1.1 Material I (E-glass/epoxy, [ $\pm 45/0_4/\pm 45/$ ])

The results of the NN fatigue life prediction for Material I are presented. For this composite, fatigue data from three sets of stress ratios of 0.1 and 0.5, 0.5 and -0.5, and 0.1 and -2 were employed as the training data sets. The selection of stress ratios represented the different conditions of fatigue state. The results of the NN fatigue life prediction are shown in Figures 5-2 to 5-4.

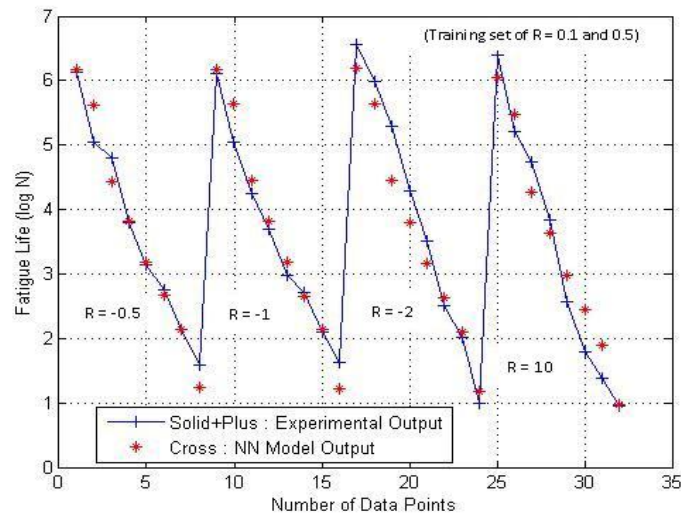


**Figure 5-2** Fatigue life prediction by NN model for testing sets  $R = -0.5, -1, -2$  and 10 using  $R = 0.1$  and 0.5 as training set.

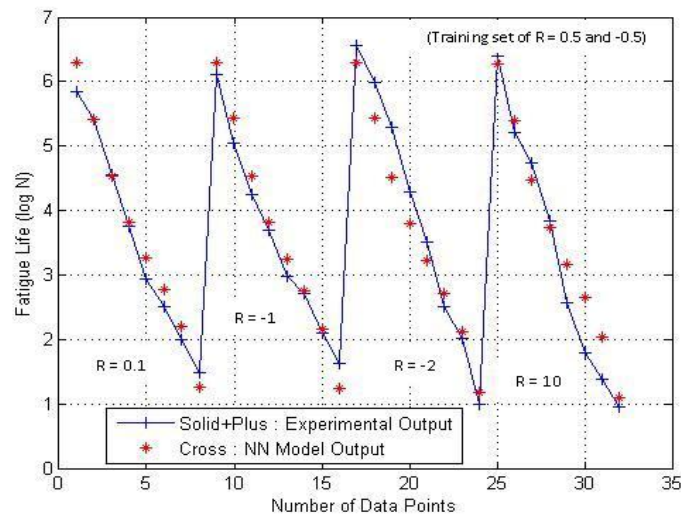


**Figure 5-3** Fatigue life prediction by NN model for testing sets  $R = 0.1, -1, -2$  and 10 using  $R = 0.5$  and -0.5 as training set.

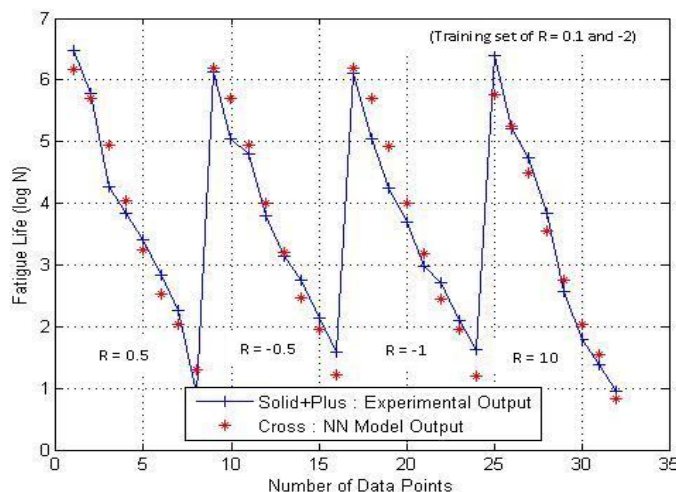


**Figure 5-4** Fatigue life prediction by NN model for testing sets  $R = 0.5, -0.5, -1$  and  $10$  using  $R = 0.1$  and  $-2$  as training set.

From Figures 5-2 to 5-4, it can be seen that the NN prediction of the material's fatigue lives are consistent with that of the experimental values. Also, the NN prediction trends closely match the experimental data trends. This means that the NN model is able to capture the necessary information and general trend of the fatigue data well during its learning phase.

The results also showed that there is no significant difference in the precision of the prediction as the training sets are varied from T-T to T-C condition mode. This is evidenced by a consistent MSE values calculated for the three different training sets as shown in Table 5-2. On average, the MSE measured for Material I is  $0.12 \pm 0.01$ . Based on the findings, the use of the training set of T-T stress ratios may be preferred compared to the training set of T-C or C-C stress ratios due to the simplicity of T-T fatigue testing. Fatigue testing under high compression condition may require the use of additional guide and supports to avoid buckling of the sample.

**Table 5-2** The MSE of the fatigue life prediction results of Material I for various training sets

| Training set | $R$ values               | The MSE prediction value |
|--------------|--------------------------|--------------------------|
| Set A        | 0.1 (T-T) and 0.5 (T-T)  | 0.12                     |
| Set B        | 0.5 (T-T) and -0.5 (T-C) | 0.13                     |
| Set C        | 0.1 (T-T) and -2 (T-C)   | 0.11                     |

From Table 5-2, it is observed that the training set of 0.1 and -2 gives the best prediction results indicated by the lowest MSE value of 0.11. Although both the training sets B and C are of the combination T-T and T-C mode, training set C gave better prediction results with lower MSE value. This may be due to the wider spread of fatigue data as demonstrated by the CLD in Figure 1-3.

For better insights, the fatigue life prediction results are also displayed in the classical  $S-N$  curve form as shown in Figures 5-5 to 5-8. The results presented are for those using  $R = 0.1$  and -2 as the training set with the lowest MSE. Similar observations apply to training sets A and B.

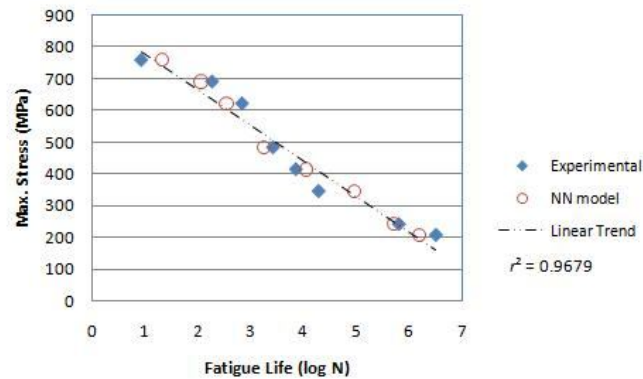


**Figure 5-5** The  $S-N$  curves based on experimental data and as predicted by the NN model for  $R = 0.5$ .

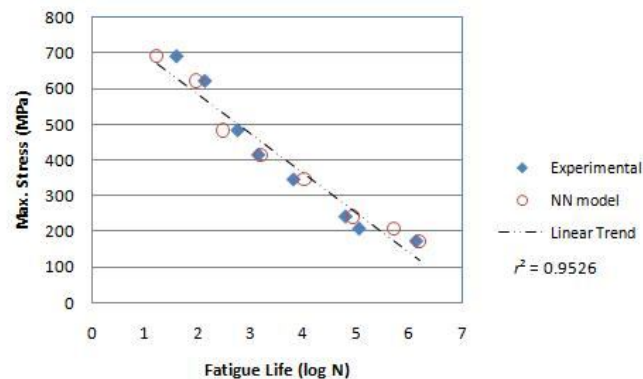


**Figure 5-6** The  $S-N$  curves based on experimental data and as predicted by the NN model for  $R = -0.5$ .

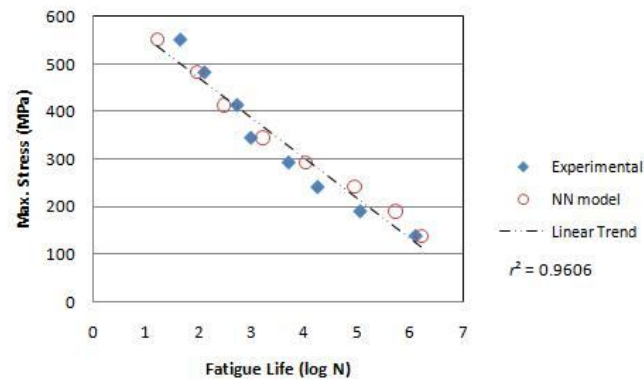


**Figure 5-7** The  $S$ - $N$  curves based on experimental data and as predicted by the NN model for  $R = -1$ .

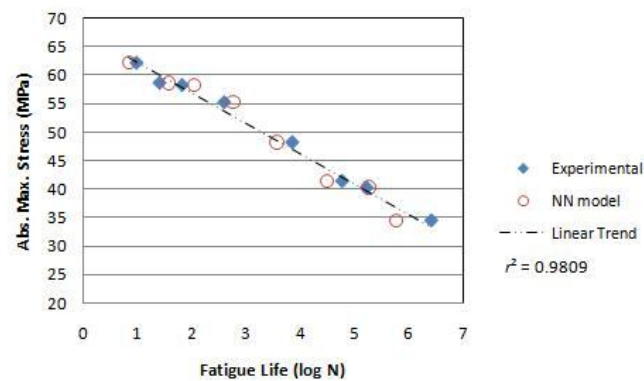


**Figure 5-8** The  $S$ - $N$  curves based on experimental data and as predicted by the NN model for  $R = 10$ .

The  $S$ - $N$  curves predicted by the NN model correlate well with those based on experimental data for all the stress ratios under study as indicated by the high coefficient of determination  $r^2$  values ranging from 0.9526 to 0.9809. Note that the discrepancies between the experimental data and the NN predicted values fall within reasonable range. The general trend observed was also justifiable.

Note that there were eight fatigue data involved at each stress ratio. In particular for Material I, there was a total of 48 fatigue data employed in the training and testing phase at six different stress ratios. As two stress ratios were used as the training set in predicting the fatigue life at other four  $R$  values, this represents 33% utilization of the

data as training examples. The utilization of the limited fatigue data as the NN training examples illustrates the value of the current study. In practice, fatigue data is indeed limited and made worse due to the very time consuming fatigue testing.

One of the most important finding from the current study is the possibility to assess and predict the fatigue life of composites at the beginning of the design or testing stage with limited fatigue data available. It has been shown that reliable and consistent prediction of fatigue life was achieved by using fatigue data at only two  $R$  values as the training set.

### 5.1.2 Material II (E-glass/polyester, [90/0/ $\pm$ 45/0]<sub>s</sub>)

In this section, the results of the NN fatigue life prediction for Material II are presented. Different from Material I where eight fatigue data were involved at each stress ratio, there were only five fatigue data at each stress ratio for this material. However, more  $R$  values are involved than those of Material I. It can be said that the NN prediction of the material's fatigue life is more challenging with lesser training examples. The NN fatigue life prediction results obtained are shown in Figures 5-9 to 5-11.

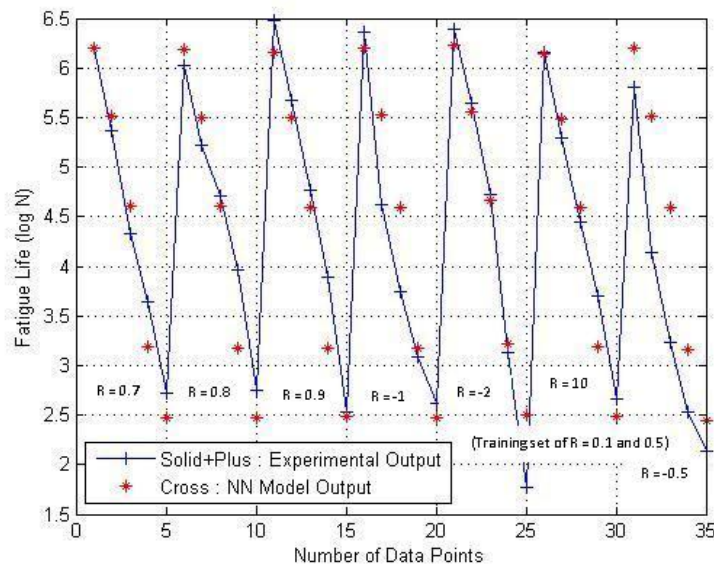


**Figure 5-9** Fatigue life prediction by NN model for testing sets  $R = 0.7, 0.8, 0.9, -1, -2, 10$  and  $-0.5$  using  $R = 0.1$  and  $0.5$  as training set.

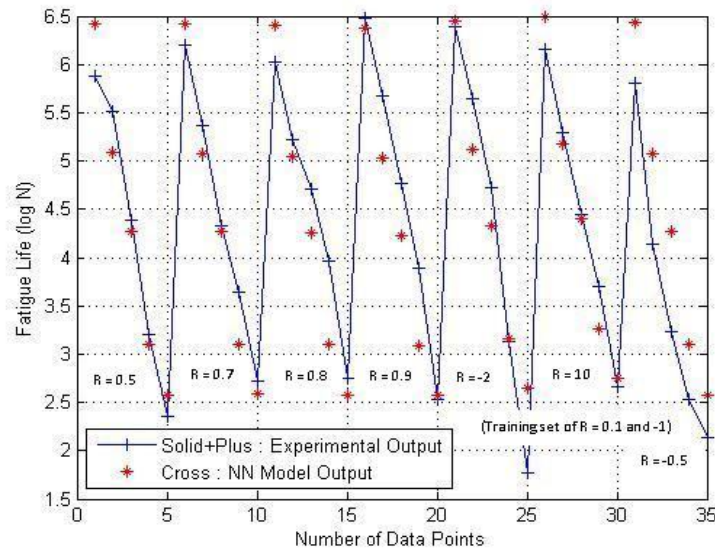


**Figure 5-10** Fatigue life prediction by NN model for testing sets  $R = 0.5, 0.7, 0.8, 0.9, -2, 10$  and  $-0.5$  using  $R = 0.1$  and  $-1$  as training set.

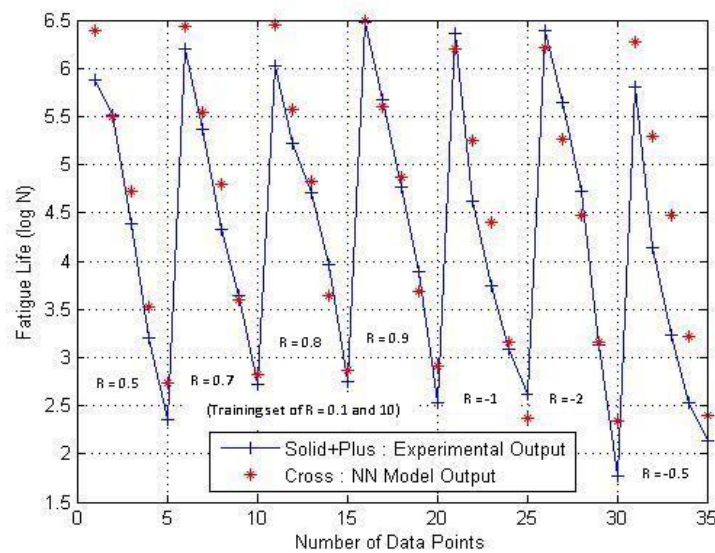


**Figure 5-11** Fatigue life prediction by NN model for testing sets  $R = 0.5, 0.7, 0.8, 0.9, -1, -2$  and  $-0.5$  using  $R = 0.1$  and  $10$  as training set.

As pointed out in Table 5-1, the NN model used to predict the fatigue life of all the three materials utilised the same number of hidden nodes of 10, thus the prediction results are comparable from material to material. For Material II, however, the number of fatigue data involved at each stress ratio is 5, which is lesser than the ones for Material I as can be seen in Figures 5-9 to 5-11. With nine stress ratios involved in total and with only two



were used as the training set, the percentage of the training samples was 22% of the total fatigue data.

From Figures 5-9 to 5-11, it is interesting that with lesser training examples, the fatigue life prediction results are generally still consistent with the experimental data, with an exception for fatigue life prediction at stress ratio  $R = -0.5$ . This indicates that the NN model was still able to deal with the more limited training examples of the Material II's fatigue data. The necessary fatigue information and regularity contained in the training examples could be captured fairly well by the NN model to produce generally consistent fatigue life prediction results. This is also indicated apparently by the  $R^2$  values shown in Figures 5-12 to 5-18.

Nevertheless, the MSE values obtained were not as high as those of Material I. The MSE values of the fatigue life prediction results of Material II for the various training sets A, B and C are summarized in Table 5-3. From Table 5-3, it can be seen that the MSE values were reduced to the lower values than those of Material I. This may happen due to the lesser examples employed as the training data set for the NN model. Also, it can be observed that there is a variation in the MSE values of the NN prediction as the training sets are varied from T-T to C-C condition mode. The variation in the MSE values range between 2% to 6%. On average, the MSE measured for Material II is  $0.22 \pm 0.03$ .

**Table 5-3** The MSE of the fatigue life prediction results of Material II for various training sets

| Training set | $R$ values              | The MSE prediction value |
|--------------|-------------------------|--------------------------|
| Set A        | 0.1 (T-T) and 0.5 (T-T) | 0.25                     |
| Set B        | 0.1 (T-T) and -1 (T-C)  | 0.23                     |
| Set C        | 0.1 (T-T) and 10 (C-C)  | 0.19                     |

Based on the MSE values measured, better prediction results were achieved when using training set of  $R$  values with far separated position in the CLD region, namely training set B and C. The position of the stress ratios in the two training sets allows the wider spread of fatigue data than that of the stress ratios in the training set A. However, the training set C with  $R$  values from two diametrically opposed sectors of the CLD (  $R = 0.1$  (T-T sector) and  $R = 10$  (C-C sector) ) gave better prediction with the lowest MSE value of

0.19 compared to the training set B. This may be explained as the training set consists of  $R$  values with symmetrical position in the CLD region. The strategic position of the stress ratios may have provided the best distribution of the fatigue information which in turn resulted in the best prediction results among the three training sets.

Furthermore, it is important to point out that for Material II more  $R$  values are involved than those of Material I, which means wider spectrum of fatigue states was handled. This clearly indicates the ability of the NN model to deal with wide spectrum of variable amplitude fatigue loading, which illustrates another value of the current study.

The corresponding  $S$ - $N$  curves of the prediction results based on training set C for Material II are presented in Figures 5-12 to 5-18.

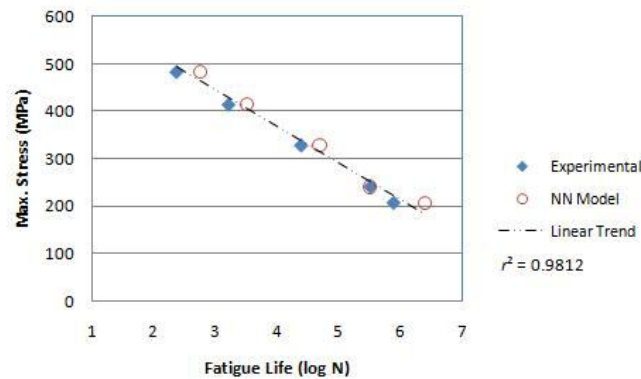


**Figure 5-12** The  $S$ - $N$  curves based on experimental data and as predicted by the NN model for  $R = 0.5$ .

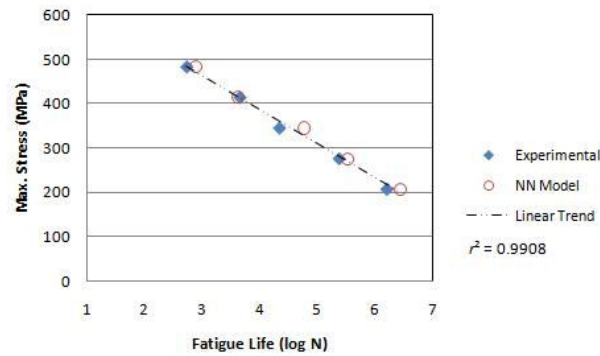


**Figure 5-13** The  $S$ - $N$  curves based on experimental data and as predicted by the NN model for  $R = 0.7$ .

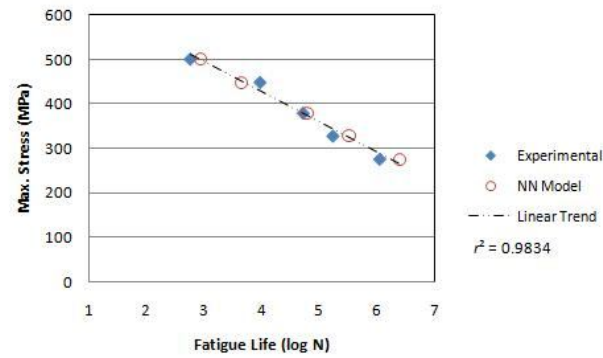


**Figure 5-14** The  $S$ - $N$  curves based on experimental data and as predicted by the NN model for  $R = 0.8$ .

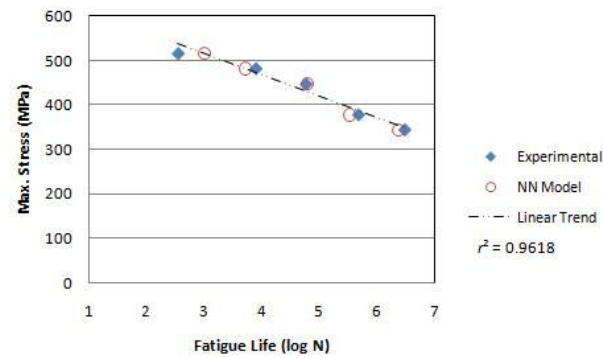


**Figure 5-15** The  $S$ - $N$  curves based on experimental data and as predicted by the NN model for  $R = 0.9$ .

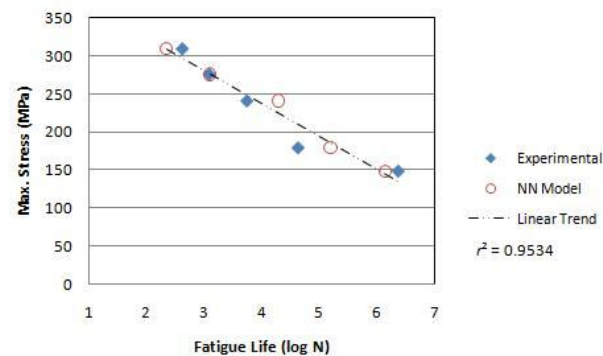


**Figure 5-16** The  $S$ - $N$  curves based on experimental data and as predicted by the NN model for  $R = -1$ .

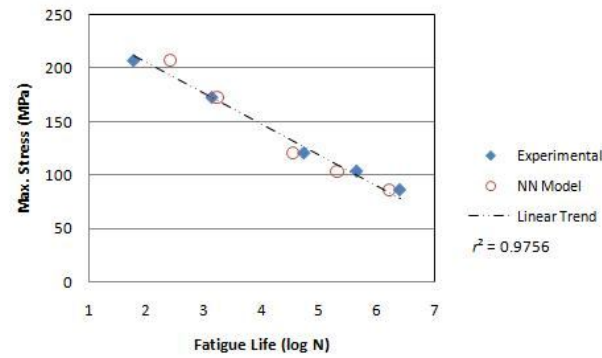


**Figure 5-17** The  $S$ - $N$  curves based on experimental data and as predicted by the NN model for  $R = -2$ .

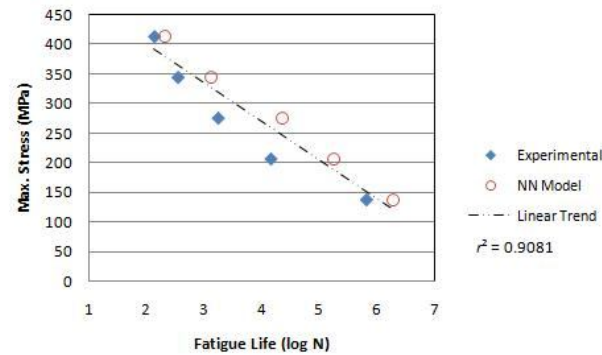


**Figure 5-18** The  $S$ - $N$  curves based on experimental data and as predicted by the NN model for  $R = -0.5$ .

As previously mentioned, the largest discrepancies in the NN fatigue life prediction compared to that of experimental data occurred at stress ratio  $R = -0.5$ , as shown by Figure 5-18. It should be pointed out that the worst prediction in fatigue life occurred at stress level between 200 – 300 MPa. At other stress level, the fatigue life prediction was consistent to that of the experimental values. On the whole, a significant value of the coefficient of determination  $r^2 = 0.9081$  was still achievable at this stress ratio. This means that the NN model still yield reasonably accurate fatigue life prediction results at stress ratio of -0.5.

Referring to the  $r^2$  values calculated, in each Figure 5-12 to 5-18, the accuracy of the fatigue life predictions of the composite can be ascertained. The highest  $r^2$  value of 0.9908 was achieved at  $R = 0.7$ , while the lowest value of 0.9081 was accomplished at

$R = -0.5$ . These findings proved that the use of 10 fatigue data as training examples which is 22% of the total fatigue data is sufficient to make a reliable fatigue life prediction of the composite.

Another significant finding of the results is that the fatigue lives predicted at lower level of maximum stress ( $\sigma_{\max} < 150$  MPa) match closely to the corresponding fatigue lives obtained from the experiment. The accuracy in low stress fatigue life prediction is useful in the context of designing components or structures to their fatigue limit or endurance limit. The endurance limit represents the largest value of stress that will not cause failure for an infinite number of cycles or infinite life. This information is of paramount importance to the design engineers.

### 5.1.3 Material III (AS4/PEEK, [0/+45/90/-45]<sub>2s</sub>)

For Material III, the fatigue data available was based on only two stress ratios, namely  $R = 0.1$  (T-T) and  $R = -0.1$  (T-C). Due to the limited data, only one training set was investigated. As previously mentioned in 4.2.3 section, in order to validate the NN model prediction, fatigue data were generated using Parametric Constant Life Method (PCLM) at four stress ratios of  $R = 0.2, -0.3, -1$  and  $10$ . These data are called simulated data.

The fatigue lives as predicted by the NN model relative to those obtained using PCLM are shown in Figure 5-19.

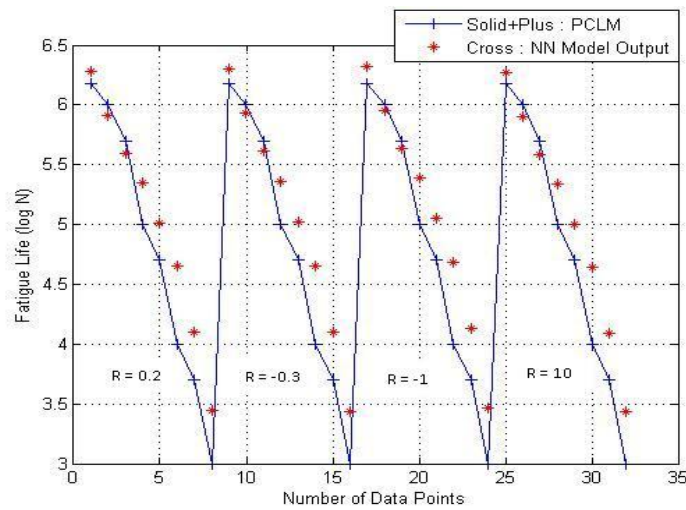


**Figure 5-19** Fatigue life prediction by NN model for testing sets  $R = 0.2, -0.3, -1$  and  $10$  using  $R = 0.1$  and  $-0.1$  as training set.

From Figure 5-19, it can be observed that the trend of prediction from both methods are consistent and comparable. In addition, generally the fatigue lives as predicted by the NN model are less-conservative relative to those predicted by PCLM. Also, the corresponding discrepancies of the fatigue lives predicted from both methods between  $10^3$  and  $10^5$  cycles are larger than those at other cycles. On the same note, the corresponding predictions at high fatigue cycles (between  $10^5$  and  $10^7$  cycles) are very close between both methods. This can be clearly observed in the corresponding S-N curves of the prediction results as shown in Figures 5-20 to 5-23, along with the  $R^2$  values of the exponential fit of both methods.

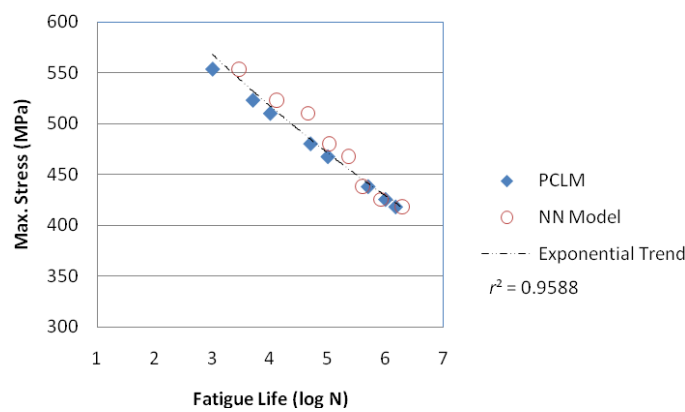


**Figure 5-20** The S-N curves based on Parametric Constant Life Method and as predicted by the NN model for  $R = 0.2$ .

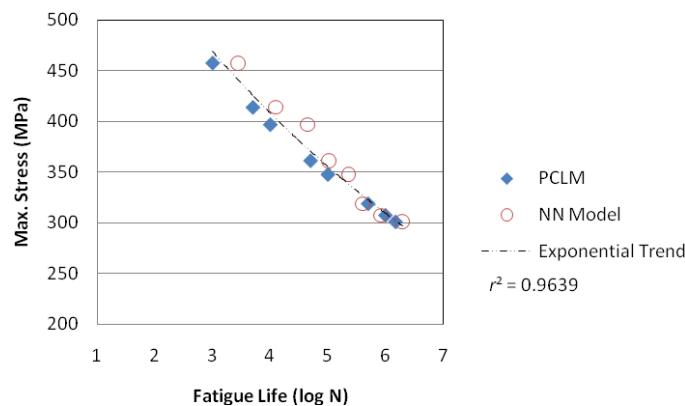


**Figure 5-21** The S-N curves based on Parametric Constant Life Method and as predicted by the NN model for  $R = -0.3$ .

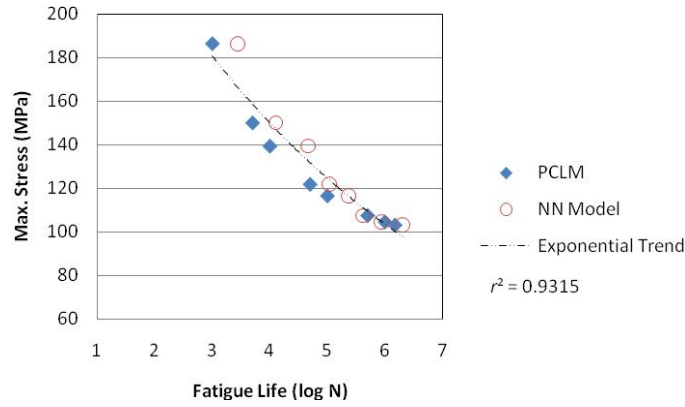


**Figure 5-22** The  $S$ - $N$  curves based on Parametric Constant Life Method and as predicted by the NN model for  $R = -1$ .

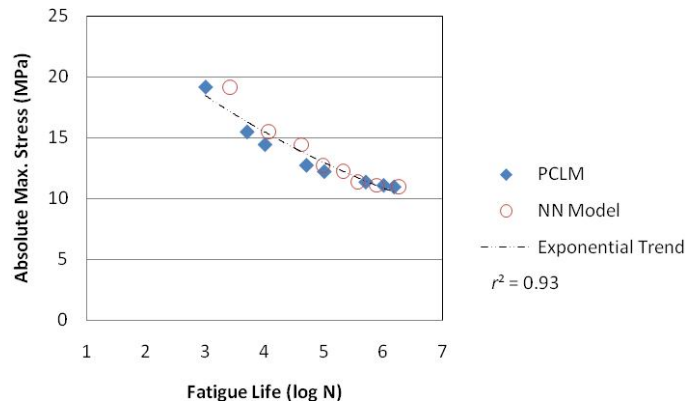


**Figure 5-23** The  $S$ - $N$  curves based on Parametric Constant Life Method and as predicted by the NN model for  $R = 10$ .

The  $r^2$  values of the exponential fit of both methods for  $R = 0.2$ ,  $-0.3$ ,  $-1$  and  $10$  are  $0.9588$ ,  $0.9639$ ,  $0.9315$  and  $0.93$ , respectively. These values are considered high and denote the strength of the exponential association between maximum stress and the predicted fatigue life.

Although both methods utilized the same experimental data and produced comparable fatigue life predictions, it should be pointed out that the results are only predictive. Further investigation and confirmation are required to examine whether the fatigue lives at those stress ratios would fall within the range of the predicted results. PCLM may be the lower bound and the NN model as the upper bound in the fatigue life prediction.

Nevertheless, modeling and simulation for this material is still important and interesting, because there is a chance to compare and assess the consistency of NN prediction to other well-known method in the fatigue field.

The consistency in the fatigue life prediction between the NN model and PCLM is measured by the MSE value as shown in Table 5-4. Note that the number of the training examples and the total fatigue data for Material III is the same with that of Material I. By considering the MSE value per se, the corresponding MSE values of the prediction results for both materials are comparable.

**Table 5-4** The MSE of the fatigue life prediction results for Material III

| Training set | <i>R</i> values | The MSE prediction value |
|--------------|-----------------|--------------------------|
| A            | 0.1 and -0.1    | 0.13                     |

#### **5.1.4 Evolution of Optimization, Regularization and NN Parameters during Iteration**

It may be interesting to see how the parameters lambda, alpha and beta as well as the effective number of parameters (weights) evolved during the NN iteration. Parameters lambda, alpha and beta refer to the optimization and regularization parameters while the effective number of parameters refers to how many number of weights were effectively used during the NN iteration which represents the effective connections between the NN layers relative to the total number of weights.

Figures 5-24 to 5-27 show the evolution of lambda, alpha, beta and the effective number of parameters during the NN iteration for Material I using training set of 0.5 and -0.5.



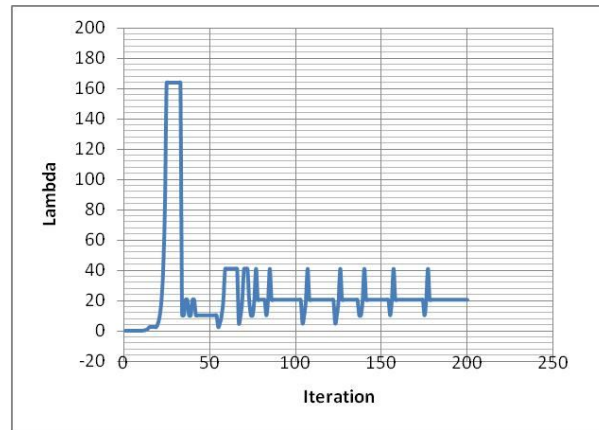


**Figure 5-24** The evolution of optimization parameter  $\lambda$  during the NN iteration for Material I.

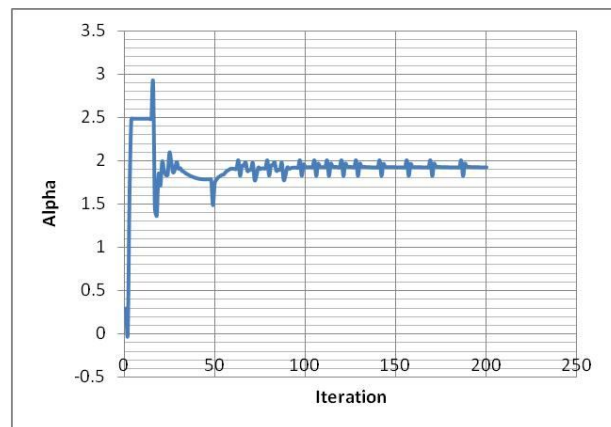


**Figure 5-25** The evolution of regularization parameter  $\alpha$  during the NN iteration for Material I.

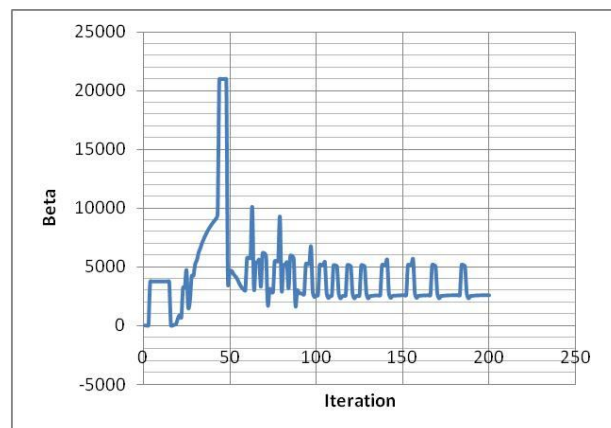


**Figure 5-26** The evolution of regularization parameter  $\beta$  during the NN iteration for Material I.

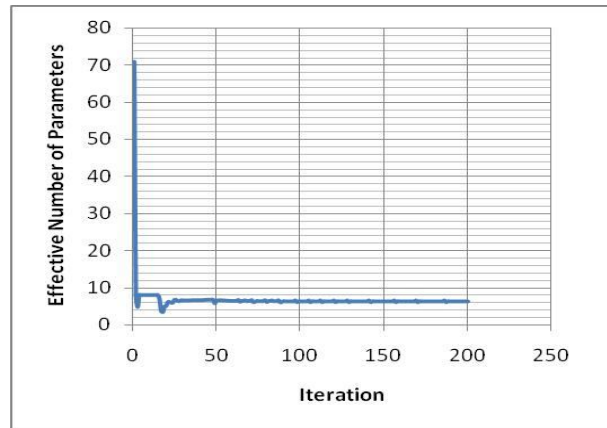


**Figure 5-27** The effective number of parameters during the NN iteration for Material I.

Figures 5-28 to 5-31 show the evolution of lambda, alpha, beta and the effective number of parameters during the NN iteration for Material II using training set of 0.1 and 0.5.

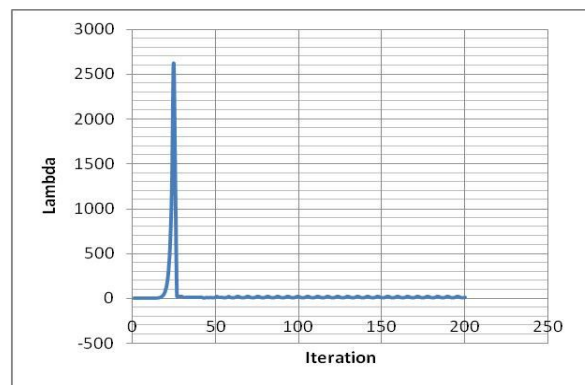


**Figure 5-28** The evolution of optimization parameter  $\lambda$  during the NN iteration for Material II.

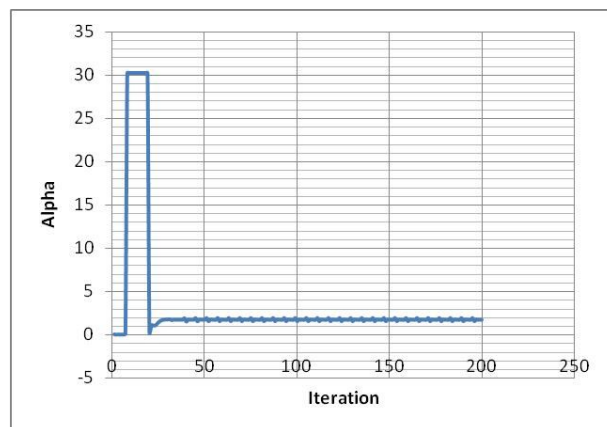


**Figure 5-29** The evolution of regularization parameter  $\alpha$  during the NN iteration for Material II.

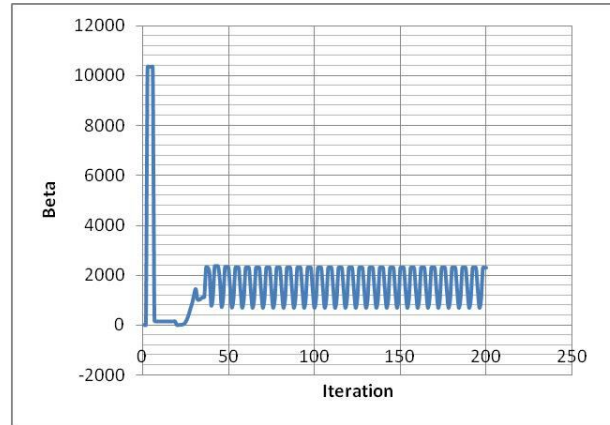


**Figure 5-30** The evolution of regularization parameter  $\beta$  during the NN iteration for Material II.

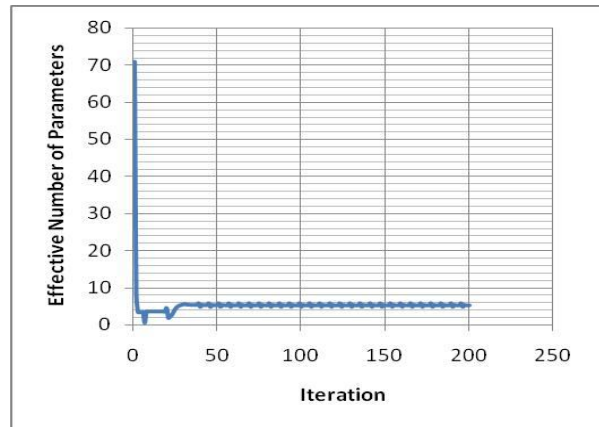


**Figure 5-31** The effective number of parameters during the NN iteration for Material II.

Figures 5-32 to 5-35 show the evolution of lambda, alpha, beta and the effective number of parameters during the NN iteration for Material III using training set of 0.1 and -0.1.

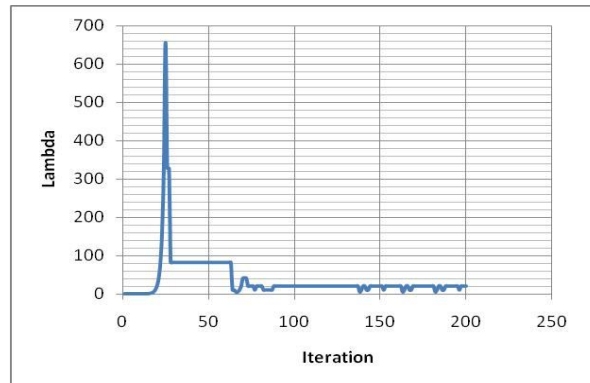


**Figure 5-32** The evolution of optimization parameter  $\lambda$  during the NN iteration for Material III.

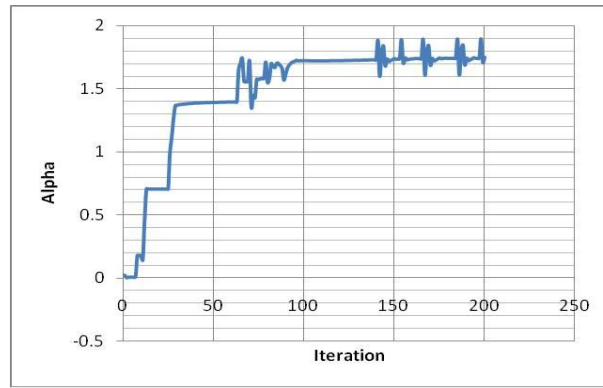


**Figure 5-33** The evolution of regularization parameter  $\alpha$  during the NN iteration for Material III.

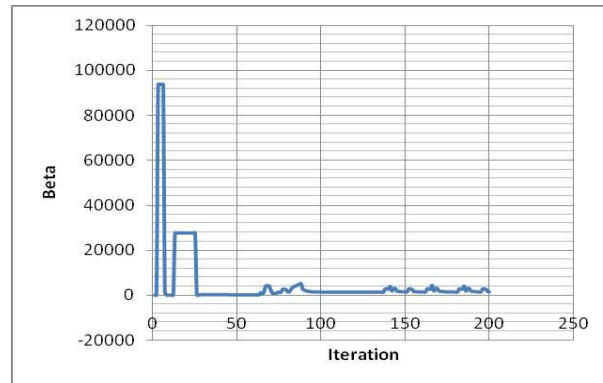


**Figure 5-34** The evolution of regularization parameter  $\beta$  during the NN iteration for Material III.

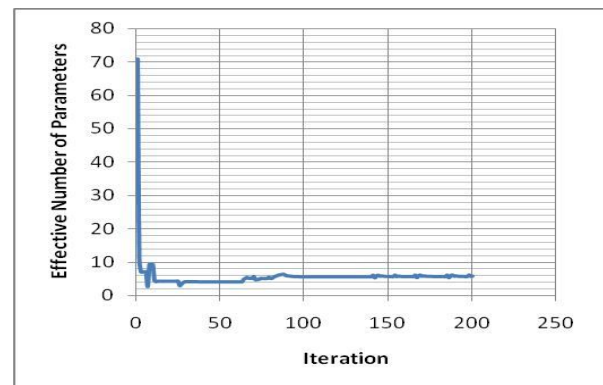


**Figure 5-35** The effective number of parameters during the NN iteration for Material III.

Note that the evolution of the NN parameters is only captured for one running and it is not always necessary that the appearance of the evolution will be the same for the subsequent runnings. The evolution depends on the initialization of the weight values

assigned randomly at the beginning of the NN iteration. Nevertheless, the general pattern of the oscillation of the NN parameters could be observed from Figures 5-24 to 5-35 that the NN parameters eventually oscillated around certain values.

In addition, for the effective number of parameters, its value tends to converge asymptotically towards a stable value of 6. Figures 5-27, 5-31 and 5-35 show that only a few weights were responsible and played dominant role in the effective connections between the NN layers. In the context of this modeling study, the few weights employed avoided over-parameterization of the NN model relative to the limited training examples and in turn contribute to better generalization performance.

### 5.1.5 Sensitivity Analysis

In the current study, the fatigue life predictions using the NN model have utilized ten hidden nodes. The number was randomly picked from a range of 2 – 30 hidden nodes (recall 4.3.3 section). Therefore, it is interesting to observe the effect of the number of hidden nodes on the fatigue life prediction results in term of the MSE values as demonstrated in Figure 5-36.

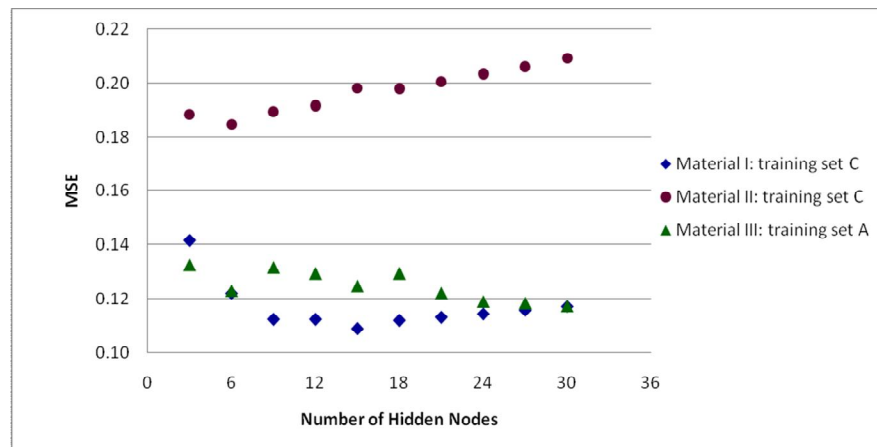


**Figure 5-36** The sensitivity of the number of hidden nodes on the MSE values.

It can be clearly seen that the number of hidden nodes of 10 was not the optimum number of hidden nodes with the smallest value of MSE. From Figure 5-36, the optimum number of hidden nodes for Material I, II and III was 15, 6, and 30, respectively.

In addition, it can be observed that for Material II which utilized less fatigue data examples as the training set, the MSE value of the NN model prediction tends to increase or the quality of the NN model prediction reduced as the hidden node number increased. This can be clearly observed in the range of hidden node number between 6 and 30. No improvement in the NN prediction quality with the increase of hidden node number indicates that there is no significant “fatigue information” could be further extracted from the training set by the NN model. This could be easily understood by considering that in principle NN works based on learning from the training examples available.

It is also important to note that the range of hidden node number examined in the current study is comparable to that employed by previous researchers. For examples Al-Assaf and El-Kadi [19], and Freire Junior et al. [21] employed a range of 8 – 23 hidden nodes, while that of 8 – 36 hidden nodes was employed by Vassilopoulos et al. [22].

## **5.2 Assessing the Quality of the NN Prediction**

In this modeling study, limited fatigue data from only two stress ratios have been employed as the training set and the corresponding fatigue life predictions, as well as the MSE values, have been presented in the previous section. In this section, the MSE values of the NN model prediction are compared to that achieved or attained by the previous researchers as a benchmark of the quality of the NN model prediction.

As previously mentioned in the literature review section, the current study is closely related to the latest works of [19-21]. In the works, at least three stress ratios were employed in the corresponding NN model as the training set. Unfortunately, the corresponding MSE value was not reported by Freire Junior et al. [21]. Therefore, the benchmark is made based on the work of Al-Assaf and El-Kadi [19], where the corresponding MSE value reported in Jarrah et al. [65] and as summarized in Table 5-5. For the current study, the lowest MSE value obtained for each material is selected for comparison.

**Table 5-5** Comparison on the MSE values obtained from previous and current studies

| Type of NN Model                                    | MSE value |
|-----------------------------------------------------|-----------|
| Previous work:<br>El-Kadi and Al-Assaf's model [19] | 0.17      |
| Current study:                                      |           |
| Material I                                          | 0.11      |
| Material II                                         | 0.19      |
| Material III                                        | 0.13      |

Referring to Table 5-5, the MSE values of the current model are lower than that of Al-Assaf and El-Kadi [19], except for Material II. Even for Material III where simulated data was employed, the MSE value achieved denotes an improved model than that utilized by Al-Assaf and El-Kadi. It is important, however, to note that the MSE value of the prediction by Al-Assaf and El-Kadi [19] was achieved by utilizing standard backpropagation algorithm with the optimum number of 12 hidden nodes, meanwhile the current study's MSE values were obtained by utilizing training algorithm of Levenberg-Marquardt with 10 hidden nodes, which is not the optimum number of hidden nodes. The optimum number of hidden nodes can be observed in Figure 5-36 with the corresponding MSE values for all the materials were 0.108, 0.185 and 0.117, respectively.

With the reasonably good MSE values obtained compared to that of the previous work, it can be said that the utilization of fatigue data from only two stress ratios as the training set is sufficient to yield reasonably accurate fatigue life predictions.

### 5.3 The Effect of Fatigue Life Scatter on the NN Model Prediction

The results of the fatigue life prediction using the NN model for the materials under study have been presented in the previous section. In general, the NN model produced reasonably accurate fatigue life predictions, where reasonably good MSE values compared to that of the previous work have been attained. Nevertheless, significant discrepancies in the prediction compared to that of the experimental values occurred at several stress ratios and/or stress levels. The discrepancies observed can be related to the

composite fatigue life scatter where the corresponding aspects and sources of the scatter have been summarized in Table 2-2. It is well-known that the fatigue life of composites is more scattered than that of metals [1].

The effect of the fatigue life scatter on the NN model prediction is now described in this section. Without loss of generality, this discussion is focused on the NN fatigue life prediction for Material II with which the MSE value obtained is the worst. In addition, more attention is given to the NN fatigue life prediction at stress ratio  $R = -0.5$  which has the lowest  $r^2$  value and in particular to the worst fatigue life prediction corresponding to the stress level between 200 – 300 MPa of the stress ratio (recall Figures 5-9 to 5-11 and 5-18).

In this modeling study, the fatigue life values used were the mean values of the corresponding scattered fatigue life. In the fatigue data base of Material II [16], a noticeable scatter happened at particular stress level(s) of  $R = 0.5, -1, -2$  and  $-0.5$ . However, the scatter of the fatigue life corresponding to the stress level between 200 – 300 MPa at stress ratio  $R = -0.5$  is more pronounced. Obviously, the great scatter of the fatigue life would result in a mean fatigue life value with a large standard deviation. In turn, this caused a significant deviation between the fatigue life obtained from experiment and that predicted by the NN model which is based on the training data set available. Although the NN model have made the generalization with respect to the new stress level inputted, it appeared that this scatter factor have affected the quality of the NN model prediction, as shown in Figures 5-9 to 5-11 and 5-18. The same argument also applies to the similar discrepancies observed at other stress ratio and/or stress level(s).

The scattering in fatigue life is unavoidable due to the inherent variability in the related aspects. It could be controlled, however, by, for examples, the use of well-maintained and calibrated fatigue testing machine, well-prepared fatigue test specimens and conducting the test carefully.